MSE307 Engineering Alloys 2014-15 L4: The Theory of Alloying

D. Dye[a]

[a]*Rm G03b, Department of Materials, Imperial College London, London SW7 2AZ, UK. david.dye@imperial.ac.uk*

In this last lecture of the introductory set we turn from selection and the phenomenology of alloy manufacture and processing, and defects, to think briefly about metal physics and how some theoretical ideas can help us when we think about alloying. This will be hard intellectual work, and I don't intend to examine it very heavily, but I want to briefly expose you to the fact that there are some underlying theoretical concepts we can use in developing alloys and thinking about alloying.

A brief aside on William Hume-Rothery (b. 1899, d. 1968). He was an Oxford chemistry graduate who moved from chemistry to metallurgy at the Royal School of Mines, Imperial College, becoming an FRS in 1937. He then returned to Oxford as a lecturer in Chemistry in 1938, helping to found the Department of Metallurgy (now Materials) in the 1950s. In the postwar period Materials Science and Engineering as a discipline was being invented, condensing out of multidisciplinary studies between scientists in physics, chemistry and metallurgy departments across the world. Thus, Hume-Rothery, whose research concerned "intermetallic compounds and the borderland between metallography and chemistry," helped form our modern conception of materials science in the UK, along with other greats like Cockroft, Cottrell, Mott, Frank and so on.

4.1. The Hume-Rothery Rules

Hume-Rothery's first set of rules concern substitutional solid solutions, and under what circumstances one atom (the solute) will easily dissolve in a solution of another (the solvent). He suggested that this would occur when

1. The atomic radii differ by $< 15\%$ (defined as the difference divided by the solvent radius),
2. they have the same crystal structure.
3. Complete solubility can occur if the valency is the same. Generally a metal will dissolve another of higher valency more readily than one of lower valency.
4. The solute and solvent should have similar electronegativity

So, if we examine data pertaining just to rules 1 and 2, Figure 2, we immediately make some interesting observations. Ti and Zr should dissolve each other. Examining the first long period of the transition metals, *fcc* Fe, Co, Ni and Cu should dissolve eacthother. In general, transition metals in the centre of the periods have the smallest atomic sizes. Al and Mg might be strange because they aren't transition metals, but actually have similar sizes. And so on.

If we turn to consider binary phase diagrams, we can see the applicability of the concept, Figure 1. Titanium, which is far from iron along the first period, depresses the melting point of iron more than atoms that are more similar to iron like V and Cr. Generally, alloying is easiest when the slope of the liquidus and solidus lines are most gentle. Similarly, Cu is less favourable that Co. So the slopes of the liquidus and solidus lines go in the order Co<Ni<Cu and Ti>V>Cr. Mn appears to be an exception, presumably due to the magnetism of both Mn and Fe. So for this example at least, the concepts appear to be of great utility in understanding how different phase diagrams appear.

Let us now turn to examine some phase diagrams and observe how these rules relate to what is actually observed in reality, Figure 3. In the titanium-niobium system we can see that, for bcc β-TI (the high temperature phase),

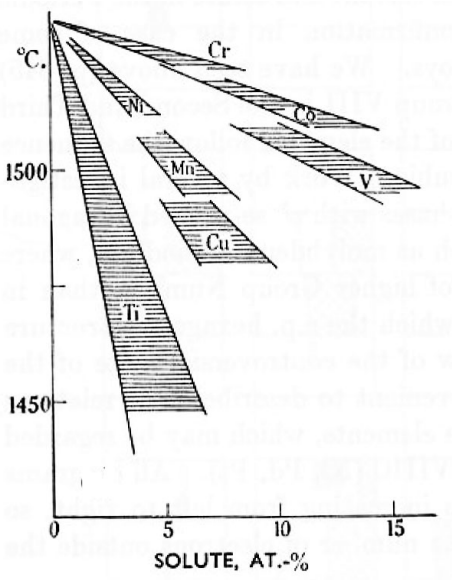

Figure 1: Liquidus and solidus lines for different solutes in (bcc) δ-Fe, from Hume-Rothery and Coles, *Atomic Theory for Students of Metallurgy*, Institute of Metals, p271, 1969.

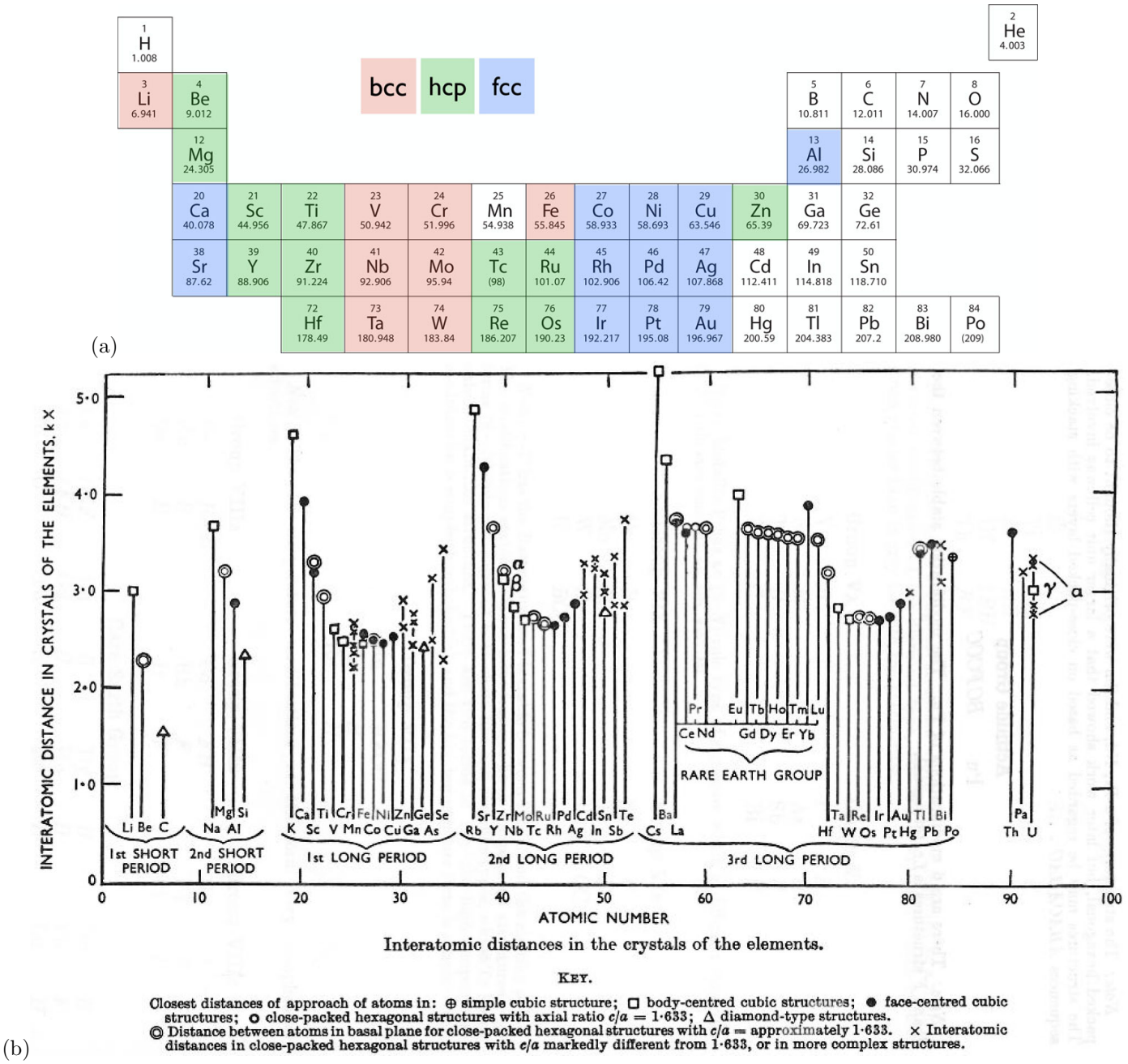

Figure 2: (a) The periodic table, showing only the elements commonly of interest for alloying, and coloured according the the room temperature crystal structure obtained for the pure metal. (b) Graph of atomic radii, with symbols according the crystal structure, from Hume-Rothery and Coles, *Atomic Theory for Students of Metallurgy*, Institute of Metals, 1969.

then there is a continuous solution with bcc Nb, but at lower temperatures then hcp α-Ti has only limited solubility for Nb.

In the Ti-Zr system, then both the bcc Ti and Zr and the hcp Ti and Zr phases have continuous solubility for each other. This can be useful, for instance in neutron scattering. Ti has a negative elastic scattering length for neutrons, whereas Zr (like most elements) has a positive scattering length. This (plus their continuous solubility for each other) means that an alloy can be produced with a net zero scattering length, and which therefore has no elastic diffraction peaks. The will be incoherent background produced from inelastic scattering, but this alloy can therefore be used in a neutron scattering beamline, e.g. as a sample holder, without producing extra irritating peaks in the diffraction pattern.

We have noted that Al and Mg are actually quite similar - both close pack, but Mg is hcp (ABAB packing) whilst Al is fcc (ABCABC packing). And so we find that Mg has the greatest solubility in Al of all the elements, and so is used as a solution strengthener in most aluminium alloys. This is limited, of course, and there are some binary

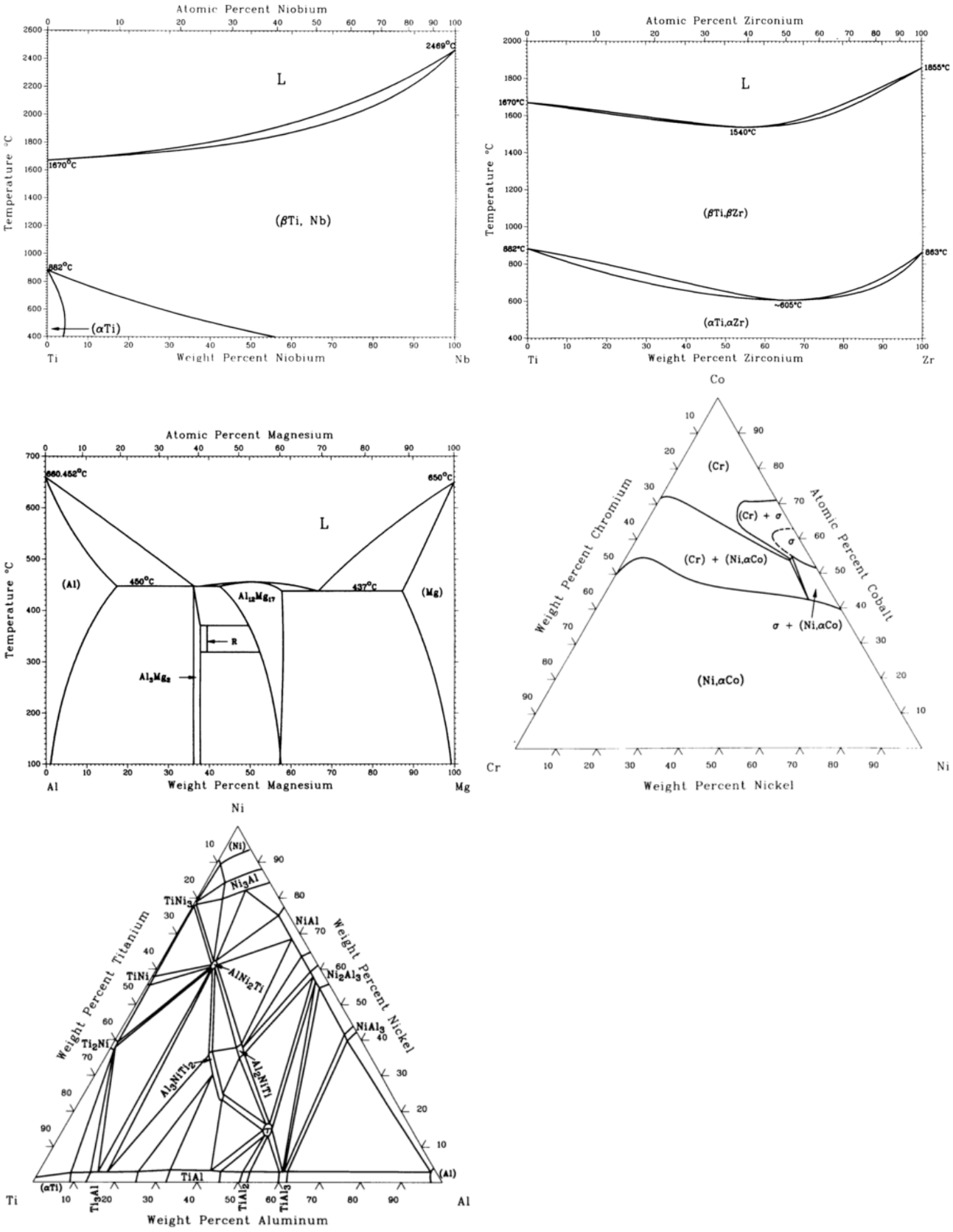

Figure 3: The Ti-Nb, Ti-Zr and Al-Mg binary phase diagrams, the Co-Cr-Ni phase diagram ternary section at 1200°C, and the Al-Ni-Ti phase diagram ternary section at 800°C. From the ASM Handbooks website.

intermetallic phases in the phase diagram.

Turning now to a ternary diagram, we examine Ni-Co-Cr. Here, Ni and Co are adjacent to each other and are both fcc (Co has an hcp phase that can form in certain circumstances, however). Therefore Ni and Co show a continuous solution, whereas both have limited solubility for Cr. Being bcc, Cr only has limited solubility for, and in, Ni and Co. This limit is of interest because Cr is commonly added to Ni superalloys (which often contain Co) in order to promote Cr_2O_3 / Al_2O_3 scale formation. If too much Cr is added then a brittle intermetallic called the sigma σ phase can form, which is a Ni-Cr intermetallic. No such phase is observed for Co, though - only α Cr is observed, which is (relatively) benign.

A more 'fun' intermetallic system is Ni-Ti-Al. Ti and Ni are different in crystal structure, so despite having similar atomic diameters (4% different - 2.8 Å for Ti and 2.7 Å for Ni) they don't show solubility for each other. And aluminium, of course, isn't a transition metal. So it isn't a surprise that these three metals have very little solubility for each other and that there are a large number of intermetallics in the system. these include the technologically interesting ones of TiAl, Ti_3Al, TiNi and $Ni_3(Al,Ti)$.

Hume-Rothery also had some rules for interstitial elements. These are elements that are so small that they can fit into the interstitial sites in the lattice. These are

1. The solute atoms must fit into the interstitial sites.
2. The solute and solvent should have similar electronegativity.

Therefore we see that H, the smallest of all atoms with an atomic diameter of 0.5 Å, has significant solubility in most metals, Bigger atoms like C, O, N and B may not and hence often form carbides and oxides instead. In titanium and zirconium, oxygen is often used to a certain extent (up to ~ 2500 ppmw) as a solution strengthener, although beyond that point, reductions in ductility can preclude further use of O strengthening.

4.2. Vegard's 'Law' and Solution Strengthening

We met Vegard's law in MSE104. In 1921, Vegard observed that the lattice parameter and solute content were usually linearly related. So, adding Al to Fe increases the lattice parameter of Fe-Al alloys in a linear fashion (notice that this isn't simply an effect of atomic diameter - Al is 2.5 Å and Fe is 2.8 Å). This isn't a physical law - we don't have a particularly solid physical rationale for this behaviour, but it does hold very commonly.

This has interesting consequences for solution strengthening in MSE203 you found that the increase in shear strength due to subsitutional solid solution strengthening, $\Delta\tau$, could be given by

$$\Delta\tau = G\delta^2 C_s \tag{1}$$

where C_s was a constant, G the shear modulus and δ the relative change in lattice parameter per at.% of solute.

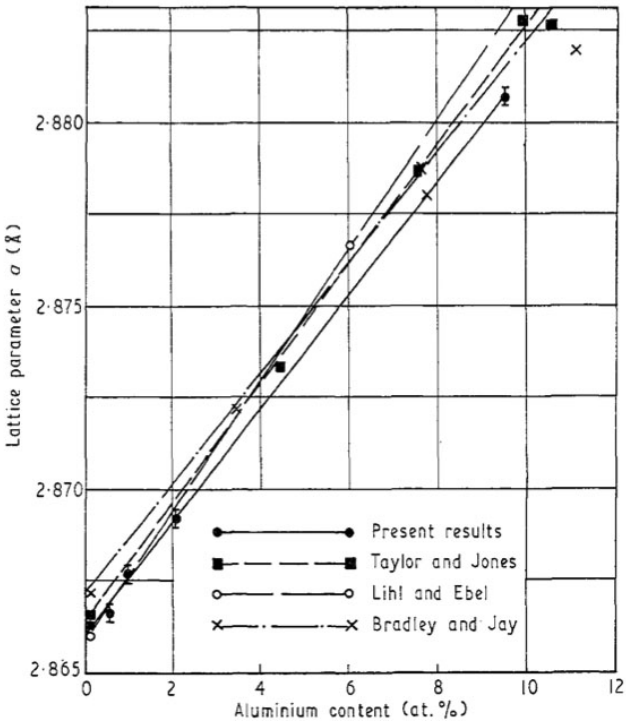

Figure 4: Illustration of Vegard's Law, showing the effect of Al solute additions on the lattice parameter of Fe alloys.

Similarly, for interstitial solid solution strengthening you found that

$$\Delta\tau = 3G\delta C_i \tag{2}$$

where C_i was a different constant. If the gradient of Vegard's law δ is assumed to arise from the difference in atomic size (average lattice expansion), then the bigger the value taken by δ, the lower the solubility of the solute will be, from Hume-Rothery's rules. Thus, we often find that the more effective the solution strengthener, the lower a solubility it has.

Some data are provided in Figure 5, which shows the hardening effect of different solutes in ferritic steels. The interstitial solutes are extremely effective but lack solubility. Moreover, the most soluble substitutional solutes, like Ni, are also the least effective.

Therefore, solution strengthening tends to be limited to strength increases of several hundred MPa, say around 300 MPa. Therefore, whilst we almost always aim to use solution strengthening in alloying, for high strength materials we are forced to rely on grain size hardening, and more especially, precipitation hardening.

4.3. Intermetallic Precipitates

A commonly used class of precipitates in Al alloys, Ni superalloys and even in steels are the A_3B precipitates with the $L1_2$ crystal structure. They are primitive cubic with the A atoms on the face centres and the B atoms on the corners of the unit cell, Figure 6(a). Technological examples include Ni_3Al in Ni, $Co_3(Al,W)$ and Co_3Ti in

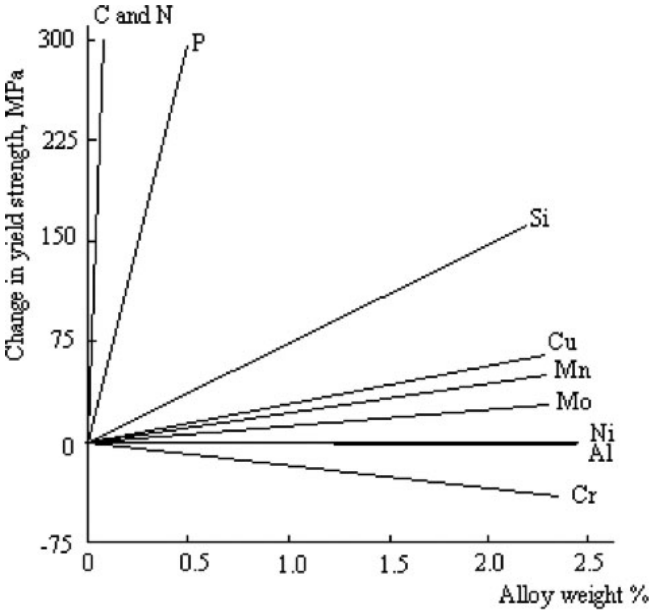

Figure 5: Hardening effect of different solutes in ferritic steels.

Co, and Al_3Li and Al_3Sc in Al. They are often found to be of very similar lattice parameter to the parent matrix of the A atom and so can precipitate coherently from the matrix, without interfacial lattice defects, at temperatures low enough that very small precipitates (10s of nm) can be developed by ageing. This means that their size can be optimised such that the can be placed at the maxima in strength due to cutting and bowing. The $L1_2$ cell can be regarded as the ordered version of the disordered matrix phases, which helps to explain why they form coherently, often by a mixed spinodal / ordering -type process.

Figure 6(b) shows an example in the Co-Al-W super-

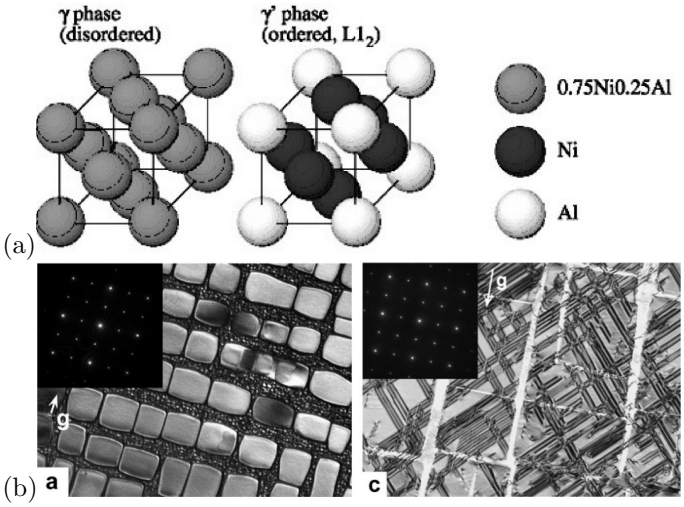

Figure 6: (a) Schematic of the Ni_3Al unit cell, as compared to the disordered fcc Ni matrix. (b) Examples of $Co_3(Al,W)$ precipitates in a Co-9Al-9W alloy (from Suzuki et al, Acta Mater, 2008). left, image of the microstructure and right, observation of APBs shearing the γ' precipitates.

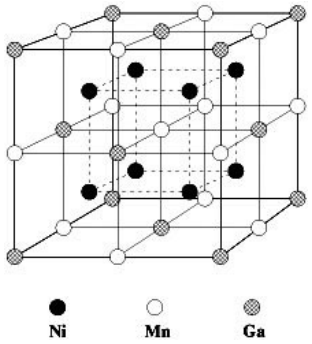

Figure 7: Sketch of the Ni_2MnGa unit cell, an example of a Heusler alloy.

alloy system. At left is an image of the microstructure in which two length scales of the γ' precipitate can be observed - so-called secondary γ' around 200 nm in size and smaller tertiary γ' that are ~ 10 nm in size.

These phases are an example of superlattice structure formed by two interpenetrating sublattices - one for the Ni sites, and another for the Al sites. It is also possible to form 3 superlattice structures. An important class of these are the Heusler alloys such as Ni_2MnGa, depicted in Figure 7. Ni_2MnGa is a shape memory alloy that can transform by shear on the application of a magnetic field or stress to a lower symmetry crystal structure. There is great interest in developing these for functional shape memory alloys for applications such as sensors and actuators.

It doesn't seem to be possible for more than three sublattices to form. This has given rise to two related technological developments in the 2000s. The first are so-called high entropy alloys, which is where 5 different elements that are not extensively soluble in each other are combined, so that when they do crystallise they form an average fcc structure, but with very high configurational entropy. The second are bulk metallic glasses. Here again, many metallic elements are combined that lack solubility with each other, and so when they are rapidly solidified they find it so hard to crystallise that a glassy state is obtained. Thus, the Hume-Rothery rules continue to be of great relevance to the hottest topics in metallurgy!

Turning back to strengthening, in MSE203, you learned that the bowing strength for a dislocation looping around hard particles was given by

$$\Delta\tau = \frac{Gb}{r}\sqrt{\frac{3f}{2\pi}} \tag{3}$$

where f was the fraction of precipitates, G the shear modulus, b the Burgers vector and r the precipitate spacing. The alternative was for the particles to be sheared by the dislocations. In the case that they provided strength due to their coherency (mismatch) strain ε, then you found that

$$\Delta\tau = \sqrt{r\frac{2k^3\varepsilon^3G^2f}{2\pi b}} \tag{4}$$

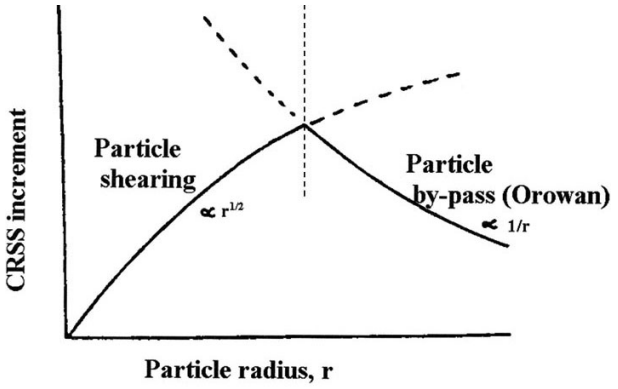

Figure 8: Sketch of the strength improvement vs precipitate size, from Martin, *Precipitation Hardening*.

where k was a constant. Where the strength was due to the formation of an anti phase domain due to a requirement to pass the matrix dislocations in pairs, then you found instead that

$$\Delta\tau = \sqrt{r\frac{12\gamma^3 f}{\pi G b^4}} \tag{5}$$

where γ was the anitphase boundary energy. Thus, large precipitates (strong) would tend to be bypassed by dislocation looping, controlled by the intrinsic strength of the dislocations, whereas small precipitates would tend to be sheared, Figure 8.

APB strengthening arises when the precipitates can be considered to be an ordered, coherent version of the matrix phase, for example, $L1_2$ precipitates in an fcc matrix. In this circumstance then, referring to Figure 6, you can observe that the perfect $\frac{a}{2}[110]$ fcc dislocation is a partial dislocation in the primitive cubic structure. Therefore, when an fcc dislocation passes through the precipitate, they produce unfavourable A-A and B-B bonds where only A-B bonds should exist (see the 2D schematic in Figure 9). This is called an antisite defect because, effectively, the two interpenetrating superlattices have been reversed. For an $L1_2$ structure the situation is more complicated, but the concept is similar. A second partial dislocation passing through the cubic primitive structure would reverse this defect, restoring the lattice, and so the region between the two partials is called an anti phase domain, or APB. The energy associated with the defect is called the APB energy and the minimisation of this pulls the partials towards each other, until that force is balanced by the repulsive force experienced between dislocations of similar sign. Thus, the picture in Figures 6 and 9 is obtained. Therefore, $L1_2$ precipitates can be extremely useful and are the basis for several alloy systems of critical importance to aviation, such as superalloys and Al-Li alloys. In Figure 9(c) a depiction of such Orowan loops decorating (rather large) precipitates is shown, illustrating the process. In such circumstances, of course both coherency and APB strengthening should be considered (for simplicity, an additive approach will usually be taken).

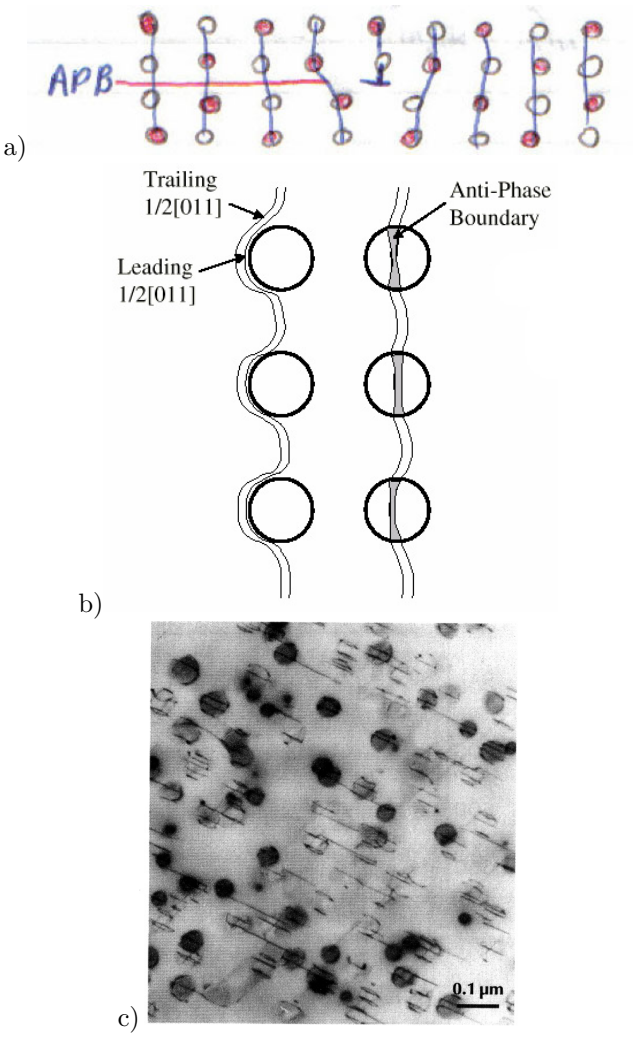

Figure 9: a) Schematic (in 2D) of the effect of a dislocation travelling left-to-right in an ordered AB structure, to produce an anti phase boundary. (b) Depiction of pairs of dislocations travelling through an ordered precipitate. (c) TEM micrograph showing Orowan loops decorating disc-shaped γ'-Ni_3Ti precipitates in a stainless steel (Figure 2.16 from Martin).

A final example of coherency and misfit between phases is the martensites, particularly in shape memory alloys (but also in steels). Consider NiTi, which has a high temperature B2 crystal structure where the Ni atoms can be found on the corners and the Ti atoms at the cube body centre. At low temperatures this can transform into a B19 orthorhombic or even a sheared B19′ monoclinic structure, by forming a distorted cell along the [110], $[1\bar{1}0]$ and [001] axes of the parent B2 phase.

If the lattice parameter differences are large to be accommodated coherently (typically they are on the order of 10%) then as the B19′ phase grows during transformation, it will generate lattice defects at its interface. This can partially be accommodated by a rotation of the lattice, and by forming twin-related (symmetrically related) pairs of martensite laths, but their interfacial strain is given by the middle eigenvalue of the distortion tensor describing

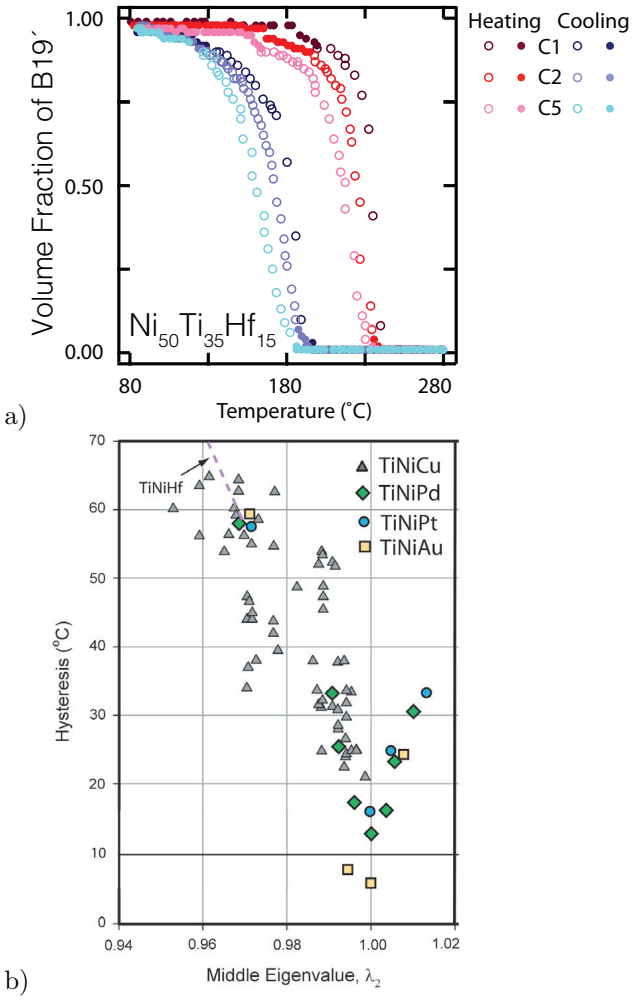

Figure 10: a) Transformation hysteresis in an NiTi alloy with cycle number C (from Azeem and Dye, Intermetallics, 2014), (b) effect of middle eigenvalue (interfacial transformation strain) on the transformation hysteresis in NiTi alloys (from Cui et al, Nature Mater, 2006).

the transformation from the old to the new lattices.

In a 2006 Nature Materials paper, RD James and coworkers used this to produce minimum-hysteresis NiTi shape memory alloys (SMAs). As can be seen for the example of NiTiHf, Figure 10(a), there is a hysteresis between the transformation temperatures from the B2→B19′ on cooling and the reverse transformation on heating. For actuator design, this is irritating, but even worse is the per-cycle drift that is also observed. It is believed that both are a result of the interfacial defects and elastic strains produced by the growth of the martensite from the austenite, because a purely thermodynamic transformation would show no such hysteresis. What RD James showed was that the hysteresis could be minimised by minimising the interface plane strain (the middle eigenvalue λ_2.

4.4. Elastic Moduli and Phonons

The elastic moduli turn out to be of great interest in understanding alloys, including why certain phases are intrinsically brittle, why some phases can shear into others on application of a stress, and in understanding spontaneous transformations. We introduced the idea that crystals might have elastic anisotropy and introduced Nye's 6×6 contracted elastic moduli C_{ij} in the MSE203 lectures on stress tensors;

$$C_{ij} = \begin{pmatrix} C_{11} & C_{12} & C_{12} & 0 & 0 & 0 \\ C_{12} & C_{11} & C_{12} & 0 & 0 & 0 \\ C_{12} & C_{12} & C_{11} & 0 & 0 & 0 \\ 0 & 0 & 0 & C_{44} & 0 & 0 \\ 0 & 0 & 0 & 0 & C_{44} & 0 \\ 0 & 0 & 0 & 0 & 0 & C_{44} \end{pmatrix} \quad (6)$$

There we found that C_{44} was the modulus relating shear stress on [100]{010} to shear strain. We also, in one of the examples, found that the shear modulus on [110]{1$\bar{1}$0} was instead given by $C' - \frac{1}{2}(C_{11} - C_{12})$.

The variation in C' as a function of the electron per atom ratio for some bcc β titanium alloys is shown in Figure 11. As vanadium is added, the e/a ratio decreases and so does C'. This is interesting, as the β phase in the world's most commonly used titanium alloy, Ti-6Al-4V, has the approximate composition Ti-20V. In addition, it was claimed in a 2003 Science paper and a follow-up Phys Rev Lett that some novel bcc Ti-Nb-based alloys (called Gum metal) deformed by ideal shear, which would become easy as C' approached zero. As it turns out, this contention was incorrect, as C', whilst low, was not as low as the density function theory (DFT) modelling had predicted. Instead the alloys are vulnerable to another instability, a shear to an orthorhombic martensite α'', and/or

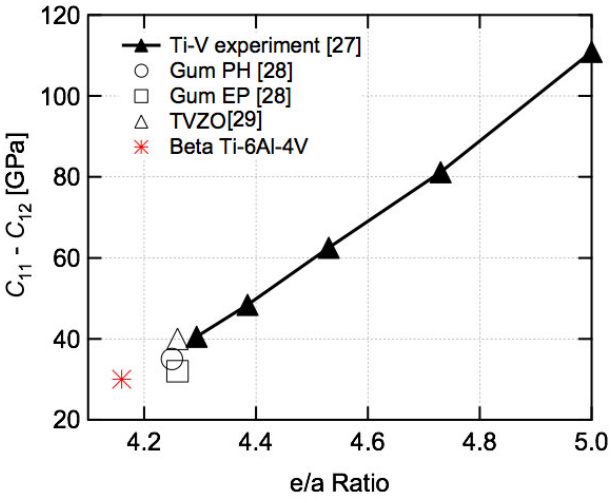

Figure 11: Variation in $C' - \frac{1}{2}(C_{11} - C_{12})$ with electron per atom ratio for bcc titanium of different compositions (From Warwick et al, Acta Mater 2012, after Collings).

twinning and the precipitation of ω phase. Thus, even something as simple as the elastic moduli can be of great interest, and debate!

There is another phenomenon that it will be valuable to consider, which are the vibrational modes of materials, termed phonons. Consider a 1D series of springs (bonds) connecting masses (atoms), where the masses i are displaced from their equilibrium positions by distances u_i and the springs have stiffness C, Figure 12. Then the restoring force F_i acting on mass i will be

$$F_i = C(u_{i+1} - u_i) + C(u_{i-1} - u_i) \tag{7}$$

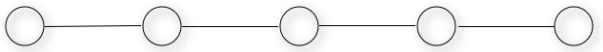

Figure 12: A series of atoms i (masses M) separated by bonds (springs) of stiffness C, with the atoms displaced from their equilibrium positions by distances u_i.

From Newton's second law $F = ma$ we can therefore say

$$M\frac{\partial^2 u_i}{\partial t^2} = C(u_{i+1} - 2u_i + u_{i-1}) \tag{8}$$

where M is the mass of the atom. This is a separable second order ODE, just like you met in high school, and in MSE101 you learned that these have (pairs of) solutions like $u_i = A\exp(-i\omega t)$. So we can say that $\partial^2 u_i/\partial t^2 = -\omega^2 u_i$ and therefore we find that

$$-M\omega^2 u_i = C(u_{i+1} - 2u_i + u_{i-1}) \tag{9}$$

Further details can be found in Kittel's *Introduction to Solid State Physics*, which is the standard 2nd year undergraduate physics text on the subject[1]. Clearly a full 3D analysis considering the longitudinal and transverse modes would be more complicated, but hopefully the general idea is clear.

Therefore materials will possess natural vibrational modes (phonons), with frequencies in the THz range, or equivalently, with energies on the order of 0-100 meV. There are $2 \times 2 = 4$ types of phonon modes that are possible - longitudinal (L) and transverse modes (T), and acoustic and optical modes. Acoustic (A) modes are coherent modes - all the atoms moving together, whereas optical modes (O) are where the movements of the atoms alternate (out of phase with each other). The optical phonons can interact with light and therefore the engineering of these is of interest for certain types of oscillators, like microwave

[1] Please don't be unduly concerned if you find this part on phonons hard going. I want to illustrate to you that there is a connection to be drawn to fairly fundamental solid state physics, not turn you into solid state physicists! I'm not intending to examine this part on phonons

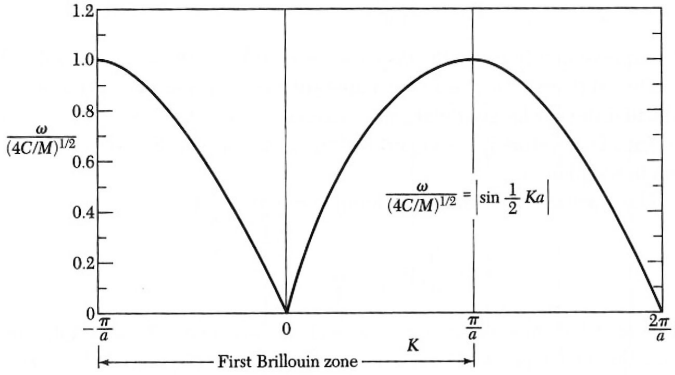

Figure 13: Calculated idealised phonon dispersion curve, showing the variation in phonon vibrational frequency with orientation (wavevector) K. From Kittel, p92.

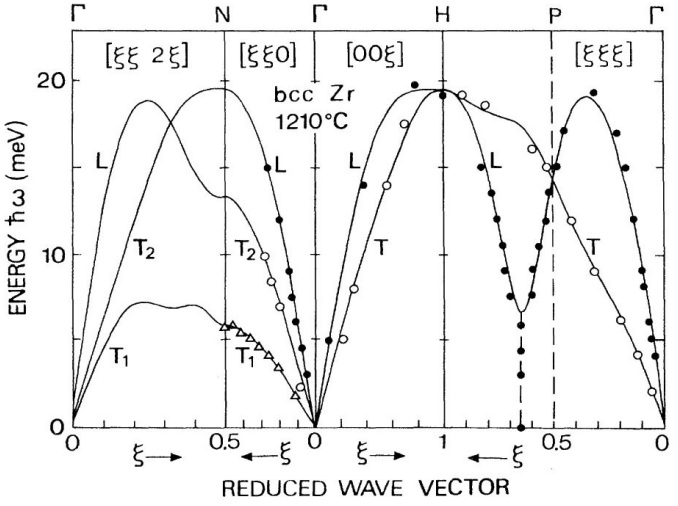

Figure 14: Phonon dispersion relation measured by triple axis neutron scattering for bcc Zr at 1210°C. From Heiming et al, Phys Rev B, 1991.

dielectrics. For the acoustic modes the phonon frequency will depend on the wave vector K, as follows

$$\omega^2 = \frac{4C}{M}\sin^2\frac{1}{K}\alpha \tag{10}$$

Therefore at the zero points (Brillouin zone boundaries or elastic scattering planes) the frequencies will be zero, as shown in Figure 13, which is termed the phonon dispersion curve. These resonances can be measured by examining the orientations at which neutrons are scattered with particular energy losses by a single crystal.

Figure 14 shows the acoustic phonon dispersion curves for bcc β Zr. Several features are apparent. The gradient of the initial curve can be used to measure the elastic constant C - high energy or 'stiff' phonon modes will have greater energy. In bcc Zr, near point P ($\{111\}$) the LA branch has an anomalous softening that wouldn't usually be observed in a bcc metal - but bcc Ti has a similar soft mode. These correspond to the vulnerability to the transformation to the ω phase, as we shall see in the tita-

nium lectures. Similarly in the Ti-Nb Gum metal alloys mentioned earlier have a soft TA2 phonon branch which corresponds to the vulnerability to shear associated with the stress-induced α'' orthorhombic martensite phase.

Phonons have a whole bunch of other applications. They are the way that heat propagates through a material, so engineering the phonon modes is important for semiconductor devices, where obtaining high rates of heat conduction is important. In addition, the vibrational modes have an associated vibrational entropy. Thus far in thermodynamics we have mainly considered configurational entropy, but in certain circumstances the vibrational entropy term can be important in stabilising a phase that would otherwise be unstable.

4.5. Blackman diagrams

Our last little study in the theory of alloys will be to return to the elastic constants and examine how their inter-relationships lead to different properties, using a tool called a Blackman diagram. These diagrams are plots for cubic materials of C_{12}/C_{11} vs. C_{44}/C_{11}, Figure 15.

We have already met $C' = \frac{1}{2}(C_{11} - C_{12})$, the $[110]\{1\bar{1}0\}$ shear modulus due to Zener. Thus, at the top axis where $C_{12} = C_{11}$, the crystal is unstable (Born's melting criterion). The straight lines fanning out from the top-right corner correspond to lines of constant shear anisotropy A (due to Zener)

$$A = C_{44}/C' \tag{11}$$

So where $A = 1$, the alloy is isotropic in shear. The bcc alkali metals (K,Na,Li) all have very high A and low C', so they are observed to easily transform from bcc to fcc.

Also shown are curved lines which correspond to the polycrystal average Poisson's ratio for an untextured aggregate. Thus, materials in the bottom right corner would have very low Poisson's ratio (auxetic), which is very unusual. Most materials have a Poisson's ratio in the range of 0.2 – 0.4.

Finally, the line running from bottom-left to top-right is the line $C_{12} = C_{44}$; materials above this line have $C_{12} > C_{44}$. $C_{11} - C_{44}$ is called the Cauchy pressure, and if it is negative then the material is found to be intrinsically brittle, because shear is easy compared to hydrostatic compression. In addition, the lower C_{12}/C_{44}, the more directional the bonding - 1 is the ideal.

Along with predictions of the fault energies and phonon curves, the elastic moduli and lowest energy crystal structures are often amenable to prediction by density functional theory, at least for stoichiometric compounds. Thus we are reaching the point where - to an extent - we can predict which materials might be ductile and strong.

Therefore the lanthanides and actinides are generally found to be brittle. The fcc metals also have similar shear anisotropy ($A \sim 3$), with the exception of a few like Al. It is noticeable that other types of compounds populate different parts of the diagram - so the transition metal carbides (NbC, VC, TiC etc) are all covalently bonded, intrinsically brittle and are in the bottom-left quadrant.

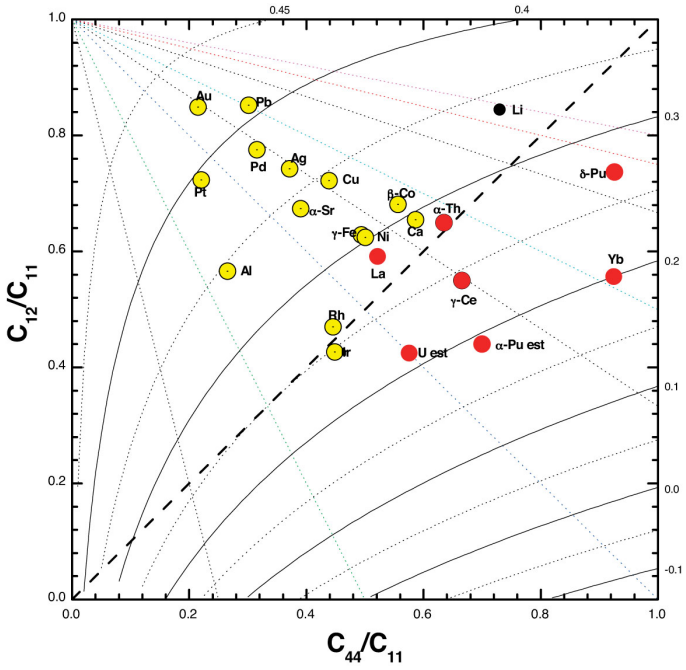

Figure 15: Blackman diagram for different fcc elements (yellow) and some lanthanides and actinides, plus Li (bcc).

4.6. Summary

In this lecture we began by examining the Hume-Rothery rules to predict when solutions would exist. This lead us onto Vegard's 'law' and the propensity for solution strengthening. The limits of this then took us onto consider intermetallic precipitates for strengthening, most particularly $L1_2$ compounds and APB strengthening. That also led us to consider structures considering more than one sublattice, including Heusler alloys. The consideration of misfit then took us on to think about martensites and their interfacial strains, and the effect of these in, e.g. NiTi SMAs. We then moved on to finish with a consideration of elastic constants and phonons, and the metal physics underlying the properties of materials.

— END OF LECTURE —